Dendrite

Sonifying diffusion-limited aggregation in the browser
Technical description, Version 1

Mazen Al-Ghoul
Department of Chemistry
American University of Beirut, Beirut, Lebanon

September 2026

Abstract

Dendrite is a single-file web page that grows a diffusion-limited aggregate (DLA) of up to 100 000 particles in real time on a black field and plays the growth as music. Every particle that settles onto the cluster is a candidate for a note: its distance from the seed sets the pitch, its horizontal position sets the stereo image, and the way it touched the cluster when it stuck selects the voice (bell, pluck, or chord). A low drone underneath opens and closes with the fraction of recent particles that landed on branch tips. Two physical parameters can be changed while the cluster is growing: the sticking coefficient p, the probability that a wandering particle stays the first time it touches the aggregate, and the particle size s, the diameter of each arriving particle in lattice cells. Because every musical parameter is derived from the structure, both changes are heard as well as seen. The page also reports a live estimate of the fractal dimension. This document describes the growth model, the sonification mapping, the dimension estimators, the rendering, the interface, and the measured effect of p and s on both the geometry and the voice mix. Version 1 documents the complete released implementation, including the expanded aubergine–blue–aqua–red–gold age palette and a mobile-safe PNG export path for iPhone and iPad Safari.

1 Overview

The page (`dendrite.html`, about 56 kB) contains all of its markup, styling, and code, and depends on nothing but two web fonts that fall back to system faces when offline. It runs in any current browser using the Canvas 2D and Web Audio [7] APIs, and links to this document from its control panel. Figure 1 shows the interface: the aggregate occupies the stage, a single control column sits on the right, and a one-line readout at the bottom left reports the particle count, the reach of the cluster, the fractal dimension estimate, the current note rate, and the mix of voices being sounded.

The design intent is to let the fractal carry all the colour. The field is true black, the interface is set in warm parchment tones with hairline separators, and the main interface accent (a pale gold) is borrowed from the newest particles of the aggregate itself. In the released Version 1 the age map deliberately passes through a saturated magenta–red–orange band immediately behind the frontier. This adds a high-contrast warm region without changing the physical meaning of colour: hue still records only order of arrival. Some morphology screenshots retained in this technical note were generated during an earlier development build using a five-stop palette. The released Version 1 changes only the age-to-hue rendering and image-export pathway relative to those screenshots, not the simulated geometry, the fractal estimators, or the sonification mapping.

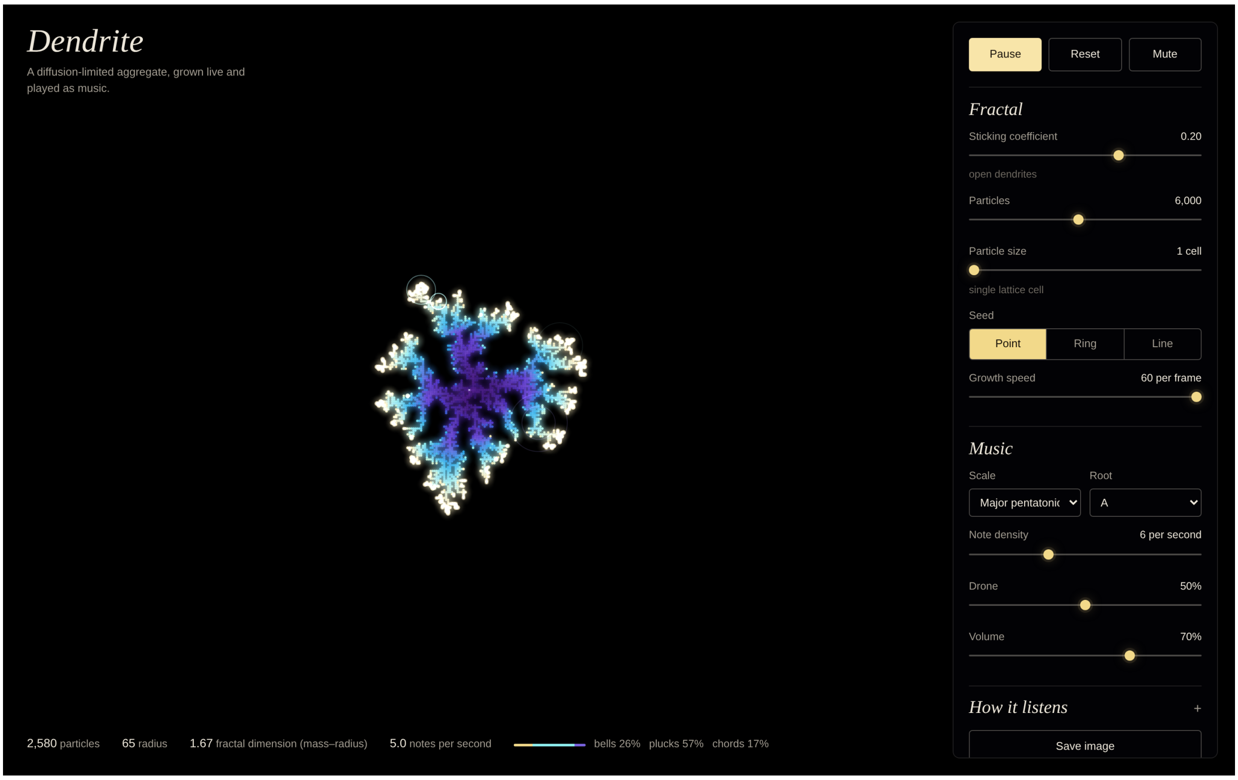

Figure 1: The page during growth with the default settings ($p = 0.20$, $s = 1$, point seed). Bright sparks mark the newest particles; faint rings expand from particles that have just sounded a note.

Experimental lineage

Dendrite grew out of our experimental program on fractal reaction–diffusion crystallization. Moon and Al-Ghoul first established a quantitative correspondence between benzoic-acid dendrites grown in gelatin and classical diffusion-limited aggregation, including fractal dimensions approaching $D \simeq 1.71$–1.74 at high supersaturation and Monte Carlo mapping of morphology onto an effective sticking coefficient [8]. A subsequent study showed that these reaction–diffusion fractal scaffolds can be conformally transmuted into the metal–organic framework HKUST-1 (MOF-199) while preserving the hierarchical fractal geometry [9]. Most recently, radial DC electric fields were shown to reproducibly tune benzoic-acid dendritic branching, crystal habit, and fractal dimension in the same soft reaction–diffusion setting [10]. Version 1 of *Dendrite* is not intended as a numerical reproduction of any one of these experiments. Rather, it is an interactive conceptual instrument inspired by this sequence of studies: the DLA picture, the sticking-coefficient control parameter, and the fractal dimension are made simultaneously visible and audible.

2 The growth model

2.1 Lattice and random walkers

Growth takes place on a square lattice of $G = 2560$ cells per side, following the original Witten–Sander prescription [1, 2]. Up to 100 000 grown particles are stored in flat typed arrays (position, diameter, contact class, growth coordinate, and time of sticking) alongside a $G \times G$ occupancy grid. One walker is active at a time; it performs a lattice random walk with four equiprobable moves until it either sticks or is discarded.

For the point seed the walker is released on a circle of radius $R_{\max} + 4 + s/2$ around the seed, where $R_{\max}$ is the current reach of the cluster, and is discarded if it wanders beyond $\min(2R_{\max} + 24,\ G/2 - 8)$. Two accelerations keep the frame rate interactive without biasing the walk. Outside the cluster, while the walker is at distance $r > R_{\max} + 3 + s/2$ from the centre, it jumps by $r - R_{\max} - 2 - s/2$ in a uniformly random direction, which cannot land it in contact with any occupied cell. Anywhere else, the lattice is also tracked at a coarse resolution of 8×8-cell blocks; if the 3×3 blocks around the walker contain no occupied cell, nothing lies within eight cells and the walker hops $7 - s/2$ cells in a random direction. Within a rendering frame the simulation is allowed a budget of 260 000 lattice operations, weighted by the size of the particle's contact shell, and stops early once the requested number of particles (the *growth speed*, 1–60 per frame) has settled.

2.2 Particle size

Each arriving particle is a disc of diameter $s \in \{1, \ldots, 6\}$ cells, rasterised as the set of cells whose centres lie within $s/2$ of the particle's centre (Table 1). For even s the centre sits on a cell corner; for odd s on a cell centre. For each diameter the page precomputes the covered cells, the ring of cells surrounding them, and, for each of the four move directions, the *leading edge*: the cells that become newly covered by the move. A move is accepted only if every leading-edge cell is empty, so particles never overlap. When the particle sticks, all of its cells are marked occupied. The size may be changed at any moment; the walker in flight is simply re-released at the new diameter, and subsequent growth proceeds at the new scale on top of the old (Figure 3(d)).

Table 1: Rasterised particle footprints. *Rim* is the number of cells in the 8-connected ring around the footprint; *facet* is the length of one flat contact (the widest edge row plus its two diagonal cells), used to normalise contact lengths in Section 2.4.

s	cells	rim	facet	shape
1	1	8	3	single cell
2	4	12	4	2×2 block
3	9	16	5	3×3 block
4	12	20	4	4×4 block without corners
5	21	24	5	5×5 block without corners
6	32	28	6	disc with rows of 4, 6, 6, 6, 6, 4

2.3 Sticking rule

After every accepted move the walker counts the occupied cells in the 4-connected shell around its footprint, n_4. If $n_4 > 0$ it sticks with probability p and otherwise keeps walking; a blocked move leaves the walker where it is. Low p therefore lets particles slide along the surface and diffuse deep into fjords before settling, which is the standard route to denser, more compact aggregates [3, 5].

```
let nb4 = 0;
for (let k = 0; k < sh4.length; k += 2) nb4 += occ(wx + sh4[k], wy + sh4[k + 1]);
if (nb4 === 0) return false;                    // not in contact
if (Math.random() >= state.p) return false;     // touched, slid off
```

2.4 Contact classes

At the moment of sticking the page walks the whole 8-connected rim of the footprint in angular order and records two numbers: the number of occupied rim cells n_8 and the number of separate contact *patches* P (maximal runs of occupied cells along the rim). The contact length is expressed in units of one flat facet for that diameter, $T = n_8/\text{facet}(s)$, and the particle is classified as in Table 2. For $s = 1$ this reproduces the natural reading of the eight-neighbour count: one neighbour is a tip, two or three contiguous neighbours are the side of a branch, and four or more, or two separated neighbours, are a crevice. For larger particles the rule asks the same question at the particle's own scale: did it touch at a point, along a face, or in two places at once?

Table 2: Contact classes derived from the rim at sticking.

Class	Rule	Local geometry	Voice
tip	$P = 1$ and $T \leq 0.5$	the end of a branch, touched at a point	bell
branch	otherwise	the side of a branch, a face-on contact	pluck
crevice	$P \geq 2$ or $T \geq 1.2$	wedged between branches	chord

2.5 Seeds

Three seed geometries are offered.

Point. A single cell at the centre; classic radial DLA.

Ring. Two concentric eight-connected circles of radius 200 and 201 cells. Growth is inward. Walkers are released just inside the innermost occupied radius r_{in}, and the empty interior is treated as a well-mixed reservoir: a walker that drifts to $r < r_{\text{in}} - 3 - s/2$ is reflected radially back to $r_{\text{in}} - 2 - s/2$. This keeps the walk confined to the annulus where the branches are and gives the coral-like inward growth of Figure 2(c).

Line. Two rows across a periodic width of 480 cells. Walkers are released four rows above the highest occupied cell and discarded if they rise forty rows above it; the lattice wraps horizontally so the growth has no edges (Figure 2(d)).

2.6 Growth coordinate

For each mode a scalar growth coordinate d measures how far a settled particle's centre is from the seed: the radius for the point seed, the inward depth $R_{\text{ring}} - r$ for the ring, and the height above the baseline for the line. The running maximum of $d + s/2$ is the reach of the cluster (the *radius*, *depth*, or *height* shown in the readout), denoted d_{max}. The normalised coordinate used by the sonification is

$$u = \min\left(1,\ \frac{d}{d_{\text{max}}}\right), \tag{1}$$

evaluated *before* d_{max} is updated, so a particle that extends the frontier has $u \approx 1$ and one that settled in a fjord has $u < 1$. Because u is relative to the current frontier, the mapping does not drift in register as the cluster grows.

2.7 Fractal dimension

The readout shows a live estimate of the fractal dimension for every seed. Both estimators operate on the set of occupied cells (excluding the seed), so particles of different sizes are weighted by their area, as they should be for a measure of the set's mass scaling.

Mass–radius regression (point seed). Occupied cells are binned by their distance from the seed, and the cumulative mass $M(r)$ is read at twelve logarithmically spaced radii between

$r_0 = \max(3,\ 0.1\, d_{\max})$ and $r_1 = 0.6\, d_{\max}$. The estimate is the least-squares slope

$$D_{\mathrm{mr}} = \frac{\mathrm{d} \ln M}{\mathrm{d} \ln r}, \qquad r_0 \le r \le r_1, \tag{2}$$

shown once the cluster has at least 200 particles and a reach of 25 cells. The lower bound avoids lattice-scale structure; the upper bound excludes the still-growing active zone. For single-cell particles at $p = 1$ the estimate settles at 1.62–1.70, close to the accepted off-lattice value of 1.71 [4], and rises towards 1.9 as $p \to 0.01$ (Section 3.7).

Box counting (ring and line seeds). Every occupied cell marks the box that contains it at box sizes $b = 1, 2, 4, \ldots, 64$; the counts are maintained incrementally, so the estimate costs nothing per frame. The estimate is the slope of $\ln N(b)$ against $-\ln b$ over $2 \le b \le E/4$, where E is the ring radius or the line width, shown once 500 particles have settled. Box counting on a finite aggregate is biased low because the smallest boxes see line-like branches, and for the ring and line seeds it measures the growth together with the one-dimensional substrate it grew from; values of 1.3–1.6 are typical.

3 Sonification

The mapping is designed so that the music is a faithful readout of the structure rather than a decoration of it: every parameter is a function of quantities the growth model already produces (Table 3).

Table 3: Summary of the structure-to-sound mapping.

Structural quantity	Musical parameter	Section
normalised growth coordinate u	scale degree (pitch)	3.1
horizontal position	stereo pan	3.2
contact class (Table 2)	voice and chord size	3.3
tip fraction of last 256 particles	drone filter cut-off	3.4
sticking events (rate-limited)	note onsets	3.5

3.1 Pitch

The user chooses a scale $\sigma = (\sigma_0, \ldots, \sigma_{L-1})$ (semitone offsets; Table 4) and a root. Three octaves of the scale are spanned from $m_0 = 48 + \text{root}$ (C3 for a root of C; the default root is A). The scale-degree index is

$$k = \min\bigl(3L - 1,\ \lfloor u^{\gamma}\, 3L \rfloor\bigr), \qquad \gamma = 2.2, \tag{3}$$

and the MIDI note is

$$m = m_0 + 12\, \lfloor k/L \rfloor + \sigma_{k \bmod L}, \qquad f = 440 \cdot 2^{(m-69)/12}\ \mathrm{Hz}. \tag{4}$$

The exponent γ spreads the near-frontier region, where most particles land, across the register: a particle at $u = 0.8$ sounds near the middle of the range rather than near the top. Frontier particles are high; particles that penetrated deep into the cluster are low.

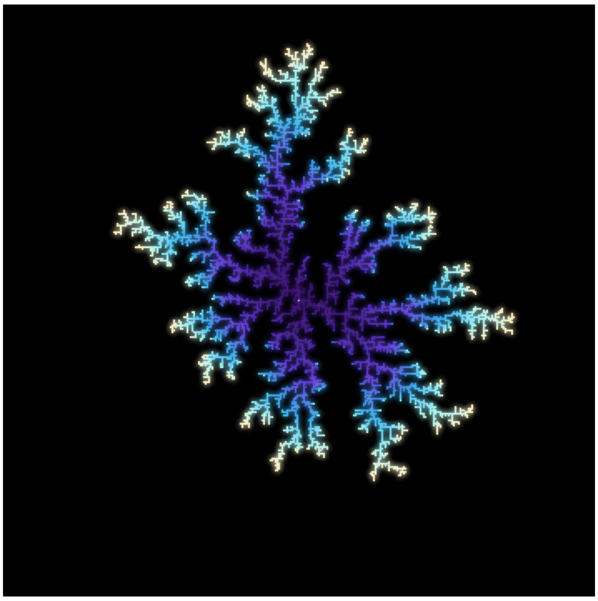

(a) Point seed, $p = 1.00$, 6 000 particles.

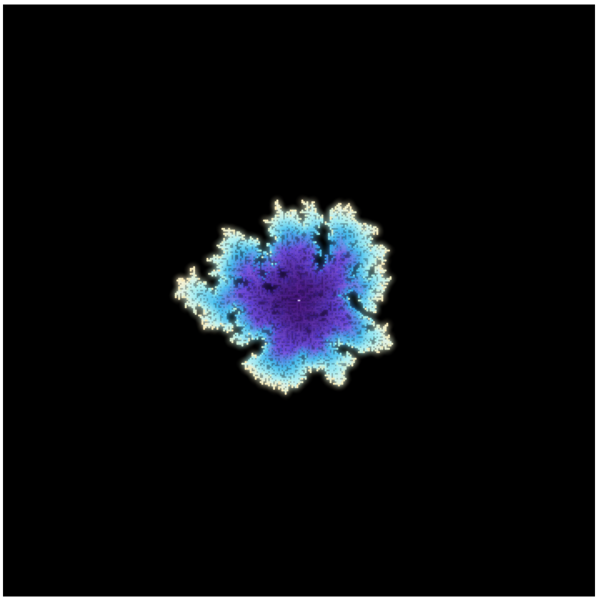

(b) Point seed, $p = 0.025$, 6 000 particles.

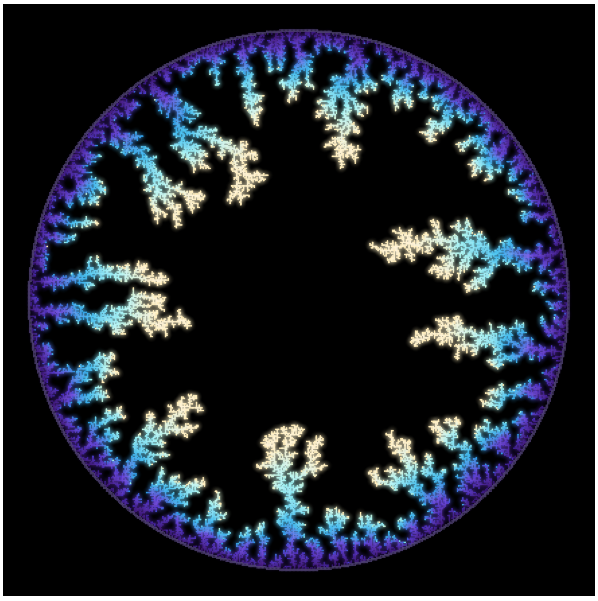

(c) Ring seed, $p = 0.20$, 20 000 particles.

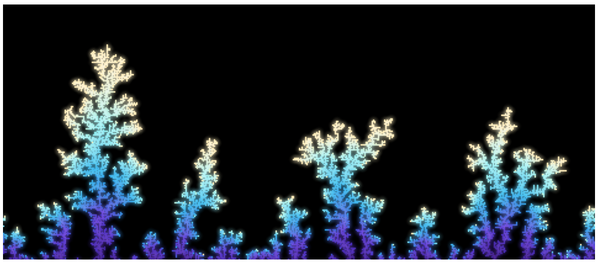

(d) Line seed, $p = 0.20$, 12 000 particles.

Figure 2: Completed aggregates of single-cell particles. The images retain an earlier five-stop development palette for morphological comparison. In the released Version 1 renderer the same arrival-order field is mapped through aubergine, violet, electric blue, aqua, magenta, vivid red, warm orange, and pale gold.

Table 4: Available scales (semitone offsets from the root).

Scale	Offsets
Major pentatonic	0, 2, 4, 7, 9
Minor pentatonic	0, 3, 5, 7, 10
Dorian	0, 2, 3, 5, 7, 9, 10
Lydian	0, 2, 4, 6, 7, 9, 11
Hirajoshi	0, 2, 3, 7, 8
Whole tone	0, 2, 4, 6, 8, 10

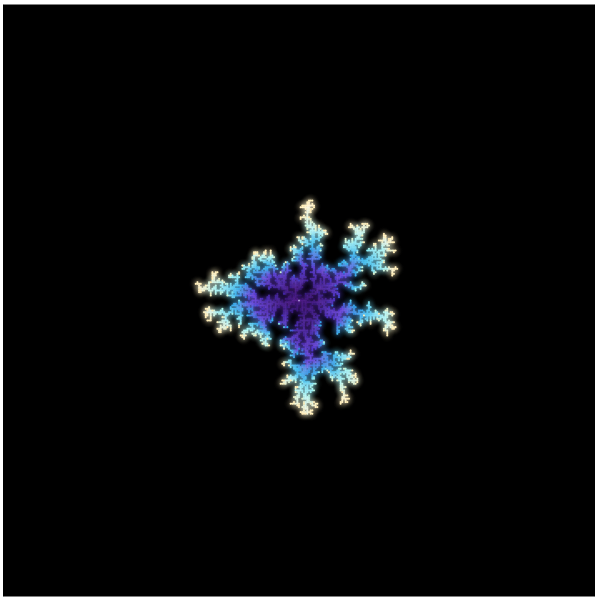

(a) $s = 1$.

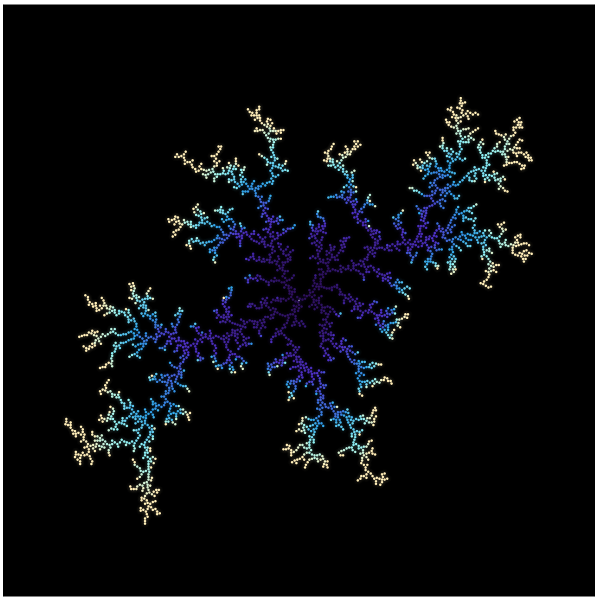

(b) $s = 3$.

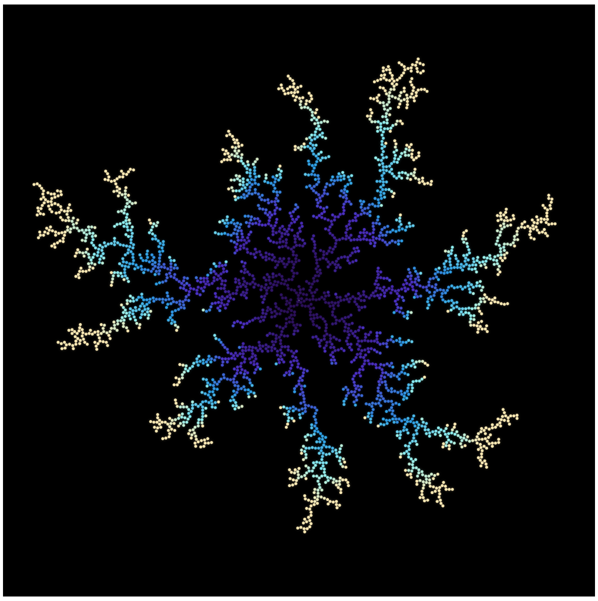

(c) $s = 5$.

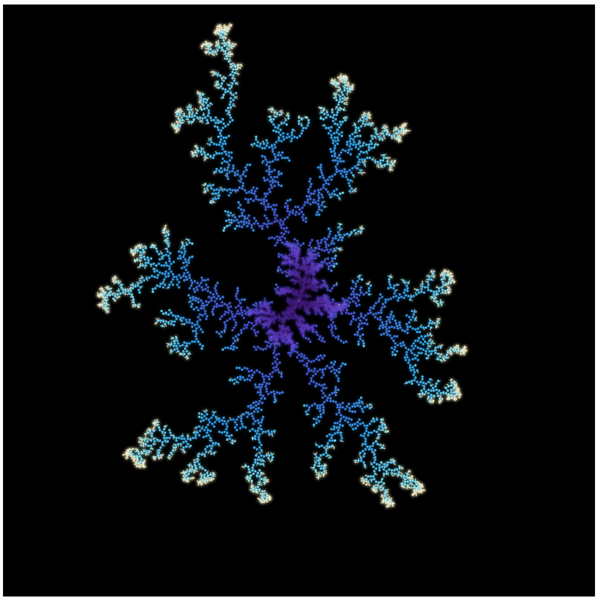

(d) Size changed during growth: 2 500 particles at $s = 1$, then 2 500 at $s = 3$, then 3 000 at $s = 1$ with p lowered to 0.025.

Figure 3: Effect of particle size at $p = 0.20$. Panels (a)–(c) are 3 000-particle aggregates; the camera pulls back as the reach grows, so the three are shown at different scales. The fractal dimension is the same to within noise; only the scale of the structure changes.

3.2 Stereo position

Sound comes from where the particle is seen. For the point and ring seeds the pan is the horizontal offset from the centre divided by $\max(d_{\max}, 12)$; for the line seed it is the offset from the middle of the periodic width. Both are clamped to $[-1, 1]$ and scaled by 0.85 to keep a little width in reserve.

3.3 Voice

The contact class of Table 2 selects one of three synthesised voices. All amplitudes below are multiplied by a velocity drawn uniformly from $[0.72, 1]$.

Bell (tip). Two-operator FM: a sine carrier at f modulated by a sine at $2f$ or $3.01f$ (chosen at random). The modulation depth starts at $\min(1.5f,\ 1400\,\text{Hz})$ and decays exponentially to $0.03f$ over 0.7 s; the amplitude rises in 6 ms and decays over 2.0 s. Peak level 0.26.

Pluck (branch). A triangle at f plus a sine at $2f$ (−13 dB) through a resonant low-pass ($Q = 1.1$) whose cut-off sweeps from $6f$ to $1.2f$ in 0.5 s; 4 ms attack, 1.0 s decay. Peak level 0.30.

Chord (crevice). A triad on scale degrees k, $k + 2$, $k + 4$, lowered by one octave. Each pitch is two triangles detuned ± 7 cents through a shared low-pass at $3.2 f_{\text{root}}$ ($Q = 0.6$); 0.25 s attack, hold to 1.1 s, release to 3.2 s. Peak level 0.11 per voice.

The consequence is that a wispy cluster, which is mostly tips, produces a sparse melody of bells, while a compact cluster, which is mostly crevices, produces sustained chords in a lower register. Large particles touch the cluster at points more often than small ones and lean towards bells unless they are wedged between branches.

3.4 Drone

A drone plays throughout on the root two octaves below m_0 (A1, 55 Hz, by default): two sawtooths detuned by -5 and $+6$ cents, a sine sub-octave, and a triangle on the fifth, the last muted automatically for scales that lack a perfect fifth (whole tone). The mix passes through a low-pass filter ($Q = 0.8$) whose cut-off follows the fraction τ of tips among the last 256 settled particles,

$$f_c = 220\,\text{Hz} \cdot 2^{3.2\,\tau}, \tag{5}$$

i.e. from 220 Hz when nothing lands on a tip to about 2 kHz when everything does, smoothed with a 0.8 s time constant and given a slow 0.07 Hz wobble of ± 55 Hz. The drone level is 0.2 times the slider value and is reduced to 45% while growth is paused or complete.

3.5 Timing

Sticking events arrive far faster than notes should. A token bucket with capacity 2 and refill rate equal to the *note density* slider (1–16 per second, default 6) decides which events sound; the rest are silent. Onsets are quantised to the next sixteenth-note slot at 92 bpm (163 ms) with a 40 ms look-ahead, at most three notes per slot (extra notes spill into the following slot), and ± 6 ms of jitter so the grid does not sound mechanical.

3.6 Space

All voices and the drone feed a dry bus (gain 0.8) and a wet bus (gain 0.5) into a convolver. The impulse response is synthesised at start-up: 3.4 s of stereo white noise smoothed by a one-pole low-pass ($\alpha = 0.28$) and shaped by $(1 - t/T)^{2.4}\, e^{-1.1t}$. The sum passes through a compressor (threshold −18 dB, knee 24, ratio 4:1, attack 5 ms, release 250 ms) and a master gain set by the volume slider. When the cluster completes, a long root chord (triad plus octave, 6 s) resolves the piece while a single ring expands from the seed.

3.7 What the two physical parameters do

Because the voices are chosen by contact geometry and the pitch by penetration depth, p and s reshape the music through the structure alone. Tables 5 and 6 and Figure 4 report headless sweeps of the page's own simulation code (point seed, four runs per value).

Sticking coefficient. As p falls from 1 to 0.01 the mass–radius dimension rises from 1.62 to 1.88, the share of tips halves, and the share of crevices rises seven-fold; the listener hears bells give way to chords and the drone close down. Changing p during growth produces a cluster whose outer shell has a different texture from its core, and the music changes character at the same moment.

Particle size. Size changes the scale of the structure, not its dimension: for $s = 1$ to 6 at $p = 0.2$ the reach of a 3 000-particle cluster grows from 76 to 624 cells while D_{mr} stays within 1.62–1.68. What the ear notices is the contact geometry. Larger discs touch at points and ring as bells more often, and chords become rarer because a big particle is seldom wedged between two branches. There is also a parity effect that belongs to the lattice rather than the physics: even diameters rasterise with flat two-cell edges, so their point contacts are two cells wide and count as tips more readily than those of odd diameters (Table 6).

Table 5: Effect of p on a 4 000-particle point-seeded aggregate of single-cell particles (mean of four runs). R is the final reach in cells; D is the mass–radius estimate of Eq. (2); the last three columns give the share of particles in each contact class, i.e. the voice mix.

p	R	D	bells (%)	plucks (%)	chords (%)
0.01	56	1.88	18	47	35
0.02	58	1.87	19	48	33
0.05	67	1.79	20	51	29
0.1	76	1.73	24	53	23
0.2	85	1.69	26	56	18
0.5	110	1.64	32	58	10
1	125	1.62	37	58	5

Table 6: Effect of particle size on a 3 000-particle point-seeded aggregate at $p = 0.2$ (mean of four runs); columns as in Table 5.

s	R	D	bells (%)	plucks (%)	chords (%)
1	76	1.62	26	56	18
2	193	1.67	78	16	7
3	325	1.64	42	53	5
4	369	1.68	61	27	13
5	480	1.64	31	60	9
6	624	1.68	47	47	6

4 Rendering

Particles are drawn once, at the moment they stick, onto an offscreen canvas of 3000 × 3000 pixels (1600 × 1600 on narrow screens) that shows a square *window* of W_c lattice cells and is composited onto the visible canvas each frame at the current zoom. For the point seed the window starts at 256 cells (about 12 pixels per cell) and doubles whenever the reach approaches its edge, up to the full lattice at about 1.2 pixels per cell; each doubling re-renders every particle, which takes a fraction of a second even for 100 000 particles. The ring and line seeds use fixed windows of 424 and 480 cells. Two marks are made per particle:

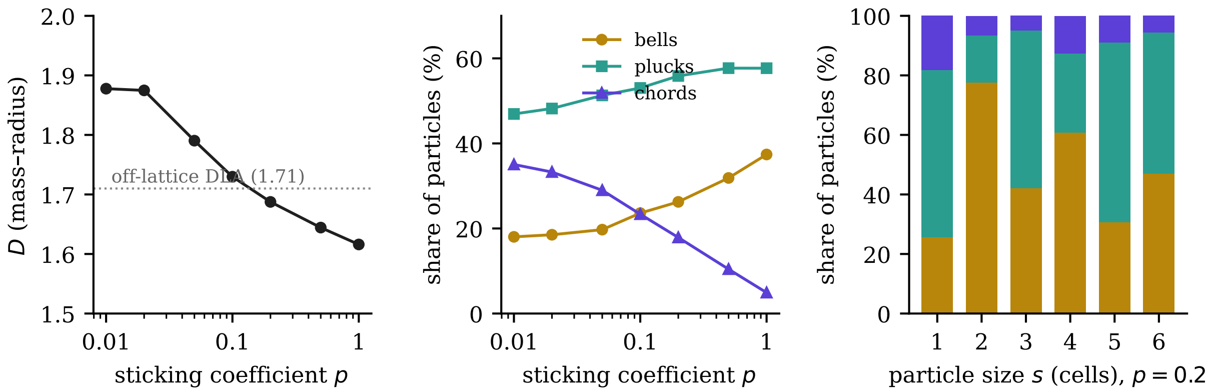

Figure 4: The sweeps of Tables 5 and 6. Left: mass–radius dimension against p; the dotted line is the accepted off-lattice DLA value. Centre: share of particles in each contact class against p, which is the share of bells, plucks, and chords in the music. Right: the same shares against particle size at $p = 0.2$; the alternation between even and odd diameters is the rasterisation parity effect.

- a soft halo, taken from a pre-rendered sprite atlas of radial gradients (one per colour; opacity 0.20 at the centre, 0.05 at 35% radius, 0 at the edge), drawn $8 + s$ cells wide and composited with the *screen* blend so that overlapping halos saturate toward their own hue rather than toward white;
- a crisp core disc of radius $\max(0.62,\ 0.48\,s)$ cells in the particle's colour, composited normally so the filaments stay legible inside the glow.

Colour encodes order of arrival: the fraction $t = (i - n_{\text{seed}})/n$ of the particle's index in the cluster is looked up in a 128-entry table interpolated linearly between the stops of Table 7. The released Version 1 palette includes magenta, vivid red, and warm orange stops between the aqua region and the pale-gold frontier. The intermediate magenta and orange anchors are important: they prevent direct aqua-to-red interpolation from passing through a visually dull, desaturated mixture and keep the warm band luminous against the black field. Because n grows, the gradient is re-normalised and the cluster re-rendered each time the count has grown by 25%, so the oldest particles remain aubergine and the newest frontier remains pale gold whatever the target count. Seed cells are drawn dim so the substrate recedes.

Table 7: Colour stops of the age gradient.

t	Hex	Name
0.00	`#2A0F57`	deep aubergine (oldest)
0.26	`#4B2FC4`	violet
0.50	`#2C9FE6`	electric blue
0.70	`#8EEFF0`	aqua
0.82	`#D7386E`	magenta bridge
0.90	`#F22E2E`	vivid red
0.96	`#FF8A2A`	warm orange
1.00	`#FFEBB5`	pale gold (newest frontier)

Three transient layers are redrawn every frame on top of the composite: *embers*, warm-white sparks on particles younger than 0.9 s that shrink and fade quadratically; *note pulses*, thin rings that expand from a particle at the instant its note sounds (0.8 s for bells and plucks, 1.5 s and a double ring for chords), coloured by voice; and the single *completion ring*. All three are suppressed when the operating system requests reduced motion.

The camera keeps the aggregate framed. For the point seed the zoom is chosen so that $R_{\max} + 14$ cells fill 45% of the stage's shorter side, clamped to between 0.35 and 4.5 screen pixels per cell and eased exponentially with a time constant of about 0.33 s, so the view pulls back smoothly as the cluster grows. The ring seed is framed at 82% of the short side; the line seed is framed by height and never zooms out beyond full-width coverage.

5 Interface

Table 8 lists the controls. Sound begins with the first press of *Grow*, because browsers require a user gesture before audio may start. The sticking slider is exponential, $p = 10^{-2+2t}$ for slider position $t \in [0, 1]$, so that the morphologically interesting decade 0.01–0.1 occupies half its travel; a caption below it names the regime in plain words (dense and mossy; thick, rounded branches; open dendrites; fine, reaching dendrites; sticks on first touch). The particle-count slider is also exponential, from 500 to 100 000, snapped to two significant figures. Changing the seed resets the cluster; changing anything else applies immediately, including during growth.

Table 8: Controls, ranges, and defaults.

Control	Range	Default	Applies
Sticking coefficient	0.01–1 (exponential)	0.20	immediately
Particles	500–100 000 (exponential)	6 000	immediately (target)
Particle size	1–6 cells	1	immediately (next particle)
Seed	point, ring, line	point	on reset
Growth speed	1–60 particles per frame	14	immediately
Scale	six scales (Table 4)	major pentatonic	immediately
Root	C to B	A	immediately
Note density	1–16 per second	6	immediately
Drone	0–100%	50%	immediately
Volume	0–100%	70%	immediately

Three buttons start or pause growth, reset, and mute. The image-export control exports a PNG of the offscreen window cropped to the aggregate. On desktop it retains the label *Save image* and uses the browser's ordinary download mechanism. On iPhone and iPad the control is relabelled *Save / Share image* and follows the iOS-specific workflow described below. Keyboard shortcuts are `Space` (grow or pause) and `R` (reset). A collapsible section, *How it listens*, explains the mapping and the two physical parameters to visitors in plain language, and a link below the controls opens this document.

5.1 Cross-platform PNG export

The exporter first renders the cropped aggregate onto a temporary canvas with a black background and serialises it as PNG. A timestamped filename is generated, for example

`dendrite-2026-09-05T17-46-00.png`

Desktop browsers then receive the image through a temporary `<a download>` element.

Mobile Safari requires a different path because synthetic download clicks are not reliably honoured on iOS. The page therefore detects iPhone/iPad (including iPadOS devices that identify as Macintosh with touch input), converts the PNG data URL into a real JavaScript `File`, checks `navigator.canShare` when available, and hands the file to `navigator.share`. This opens the native iOS Share Sheet, from which the user can choose *Save Image*, *Save to Files*, AirDrop, or another compatible destination. If file sharing is unavailable or fails for a reason other than user cancellation, the page opens the PNG in a dedicated black-background view with explicit touch-and-hold instructions. Thus the software does not attempt to bypass the iOS sandbox; it delegates the final destination to the operating system while still providing a usable fallback.

```
if (isIOS && navigator.share) {
  const file = dataURLToFile(dataURL, filename);
  if (!navigator.canShare || navigator.canShare({ files: [file] }))
    await navigator.share({ files: [file], title: 'Dendrite' });
}
```

The readout reports, live: the number of settled particles; the reach $d_{\max}$ (labelled radius, depth, or height by seed); the fractal dimension of Section 2.7, labelled with the estimator in use; the measured note rate over the last two seconds; and a three-segment bar with the share of bells, plucks, and chords among the last 256 particles. When growth stops the readout says why (target reached, or the cluster reached the edge of the field) and what to do next.

Below 820 px of viewport width the control column becomes a bottom sheet, the readout moves under the title, and the stage is the space between them. Interactive elements have visible focus rings, the seed selector is an ARIA radio group, and all sliders have labelled values.

6 Implementation notes

Structure. The file has three parts: a style sheet driven by a handful of CSS custom properties (ink, hairline, accent, panel), the markup of the stage, title, readout, and control panel, and a single self-contained script. The script holds the lattice and particle stores, the footprint tables, the walker, the dimension estimators, the renderer, the audio graph, the frame loop, and the control bindings.

Frame loop. Each animation frame runs the simulation for its budget, checks whether the render window or the colour normalisation needs a re-render, refills the note token bucket, eases the zoom, redraws the composite and transient layers, and every 160 ms refreshes the readout and the drone filter target.

Audio graph. Voices and drone $\rightarrow$ stereo panners $\rightarrow$ dry and wet buses $\rightarrow$ (convolver) $\rightarrow$ compressor $\rightarrow$ master gain $\rightarrow$ destination. Every note is a short-lived sub-graph of oscillators and gains that is scheduled ahead of time and stops itself, so there is no voice management to do.

Performance and memory. The two jump rules make the cost of a walk roughly independent of cluster size, and the operations budget bounds the worst-case frame cost at very low p or large s. In headless tests the simulation settles 100 000 single-cell particles at $p = 1$ in about twenty seconds of compute. Drawing is incremental, so the cost per frame is one large `drawImage` plus the transient marks; the occasional full re-render is the only hitch. The occupancy grid takes 6.5 MB, the box-counting marks 8.7 MB, and the offscreen canvas about 36 MB on desktop.

Embedding. Host `dendrite.html` and `dendrite.pdf` side by side and link to the page, or embed it:

```
<iframe src="dendrite.html" width="100%" height="720"
        style="border:0;background:#000" allow="autoplay"
        title="Dendrite: diffusion-limited aggregation as music"></iframe>
```

Fonts (Bodoni Moda and Albert Sans) load from Google Fonts and fall back to system serif and sans faces. The interface palette is edited in the `:root` block of the style sheet; the structure age palette is defined independently by the eight-entry `STOPS` array documented in Table 7. The iOS export path depends on Web Share support when available but retains the image-view fallback when it is not.

7 Limitations

The square lattice imprints a weak four-fold anisotropy on very large point-seeded clusters, a known property of on-lattice DLA, and the parity effect of Section 3.7 is another lattice artefact. Large particles reach the edge of the field long before 100 000 of them have settled; the page stops and says so. The mass–radius estimate is a finite-size proxy, and for a cluster grown with several sizes it reports the scaling of the composite set, which need not match either component. The ring seed's reflecting inner boundary is an approximation to a uniform source and is chosen for speed and appearance rather than fidelity. Finally, the token bucket samples sticking events uniformly, so at high growth speeds most particles are silent; the readout's voice mix is computed from all recent particles, not only the sounded ones, and therefore reports the structure rather than the sample. On iOS, saving to Photos or Files remains an explicit user action mediated by the Share Sheet; browser security rules intentionally prevent the page from silently writing into those destinations.

Revision history

Version 1 (September 2026). First public release. The implementation includes point, ring, and line seeds; a live sticking coefficient; particle diameters from 1 to 6 lattice cells; up to 100 000 grown particles on a 2560^2 lattice; coarse-block acceleration and a windowed offscreen renderer; live mass–radius or box-counting fractal-dimension estimates; structure-derived bell, pluck, chord, and drone sonification; the eight-stop aubergine–violet–blue–aqua–magenta–red–orange–gold age palette; and cross-platform PNG export with native iPhone/iPad Share Sheet support and a touch-and-hold fallback.

References

[1] T. A. Witten and L. M. Sander, "Diffusion-limited aggregation, a kinetic critical phenomenon," *Phys. Rev. Lett.* **47**, 1400 (1981).

[2] T. A. Witten and L. M. Sander, "Diffusion-limited aggregation," *Phys. Rev. B* **27**, 5686 (1983).

[3] P. Meakin, "Diffusion-controlled cluster formation in 2–6-dimensional space," *Phys. Rev. A* **27**, 1495 (1983).

[4] T. C. Halsey, "Diffusion-limited aggregation: a model for pattern formation," *Physics Today* **53**(11), 36 (2000).

[5] T. Vicsek, *Fractal Growth Phenomena*, 2nd ed. (World Scientific, Singapore, 1992).

[6] T. Hermann, A. Hunt, and J. G. Neuhoff (eds.), *The Sonification Handbook* (Logos, Berlin, 2011).

[7] P. Adenot and H. Choi (eds.), *Web Audio API*, W3C Recommendation (2021), `https://www.w3.org/TR/webaudio/`.

[8] S. Moon and M. Al-Ghoul, “Tunable Fractal Morphogenesis in Reaction-Diffusion Crystallization: From Dendrites to Compact Aggregates,” *ACS Omega* **10**(34), 38629–38639 (2025), https://doi.org/10.1021/acsomega.5c03338.

[9] S. Moon and M. Al-Ghoul, “Fractal MOF Architectures: Reaction–Diffusion–Mediated Transmutation of Crystalline Scaffolds,” *CrystEngComm* **27**, 7282–7286 (2025), https://doi.org/10.1039/D5CE00700C.

[10] S. Moon and M. Al-Ghoul, “Electric-field tuning of fractal crystallization in gelatin-based benzoic acid reaction-diffusion systems,” *RSC Advances* (2026), https://doi.org/10.1039/D6RA03214A.